Hierarchically Self-Assembled Supramolecular Host-Guest Delivery System for Drug Resistant Cancer Therapy

Hongwei Cheng[†#], Xiaoshan Fan[‡#], Xiaoyuan Wang[1], Enyi Ye[§], Xian Jun Loh[§], Zibiao Li[*§], Yun-Long Wu[*†]*

† Fujian Provincial Key Laboratory of Innovative Drug Target Research and State Key Laboratory of Cellular Stress Biology, School of Pharmaceutical Sciences, Xiamen University, Xiamen 361102, China.

‡ Collaborative Innovation Center of Henan Province for Green Manufacturing of Fine Chemicals, Key Laboratory of Green Chemical Media and Reactions, Ministry of Education, School of Chemistry and Chemical Engineering, Henan Normal University, Xinxiang, 453007, China.

§ Institute of Materials Research and Engineering, A*STAR (Agency for Science, Technology and Research); 2 Fusionopolis Way, Innovis, #08-03, Singapore 138634, Singapore.

[#] The two authors made equal contribution to this work.

Correspondence should be addressed Y.-L. Wu (wuyl@xmu.edu.cn); Z. Li (lizb@imre.a-star.edu.sg); X. J. Loh (lohxj@imre.a-star.edu.sg).

KEYWORDS: cancer therapy; MDR1; drug resistance; cyclodextrin; drug delivery.

ABSTRACT: In this report, a new star-like copolymer β-CD-*g*-(PNIPAAm-*b*-POEGA)$_x$ consisting of a β-CD core, grafted with temperature-responsive poly(N-isopropylacrylamide) (PNIPAAm) and biocompatible poly(oligo(ethylene glycol) acrylate) (POEGA) in a block copolymer of the arms, was used to deliver chemotherapeutics to drug resistant cancer cells and tumors. The first step of the self-assembly process involves the encapsulation of chemotherapeutics through host-guest inclusion complexation between the β-cyclodextrin cavity and the anti-cancer drug. Next, the chain interaction of the PNIPAAm segment at elevated temperature drives the drug-loaded β-CD-*g*-(PNIPAAm-*b*-POEGA)$_x$/PTX inclusion complex to hierarchically self-assemble into nanosized supramolecular assemblies at 37 °C, whereas the presence of poly(ethylene glycol) PEG chains in the distal end of the star-like copolymer arms impart enhanced stability to the self-assembled structure. More interestingly, this supramolecular host-guest nanocomplex promoted the enhanced cellular uptake of chemotherapeutics in MDR-1 up-regulated drug resistant cancer cells, and exhibit high therapeutic efficacy for suppressing drug resistant tumor growth in in vivo mice model, due to the increased stability, improvement in aqueous solubility, enhanced cellular uptake and partial membrane pump impairment by taking the advantage of PEGylation and supramolecular complex between this star-like copolymer and chemotherapeutics. This work signifies that temperature-sensitive PEGylated supramolecular nanocarrier with good biocompatibility are effective in combating MDR-1 mediated drug resistance in both *in vitro* or *in vivo* models, which is of significant importance for the advanced drug delivery platform designs to combat drug resistant cancer.

1. INTRODUCTION

Chemotherapy as well as cancer patient compliance have been greatly hindered by drug resistance, which is mainly mediated by membrane pump transporter related intracellular drug molecule efflux.[1-13] To be mentioned, MDR1 (P-glycoprotein) plays an important role in pump related multiple drug resistance, in terms of increasing effluent drugs.[14-17] In this case, a number of MDR1 inhibitors (i.e. verapamil, tamoxifen, quinidine) were co-delivered with anticancer drugs but were largely hampered in clinical trials due to side effects of those inhibitors.[18] Interestingly, nanoformulations, referring to delivery of anticancer drug in liposomes, polymeric nanoparticles, or inorganic nanoplatforms, can be uptake by endocytosis and lead to deep transportation in cells.[19-31] To be mentioned, poly(ethylene glycol) (PEG) modified or PEGylated polymer based nanoscale delivery systems, including nanoparticles made of Pluronic (a copolymer of PEG and poly(propylene glycol) (PPG)) or PEG-PEI copolymer with PEG and poly(ethylene imine) (PEI) blocks, were reported to deplete adenosine triphosphate (ATP) or impair MDR1 related energy dependent drug efflux.[32] In this case, they could exhibit significant therapeutic effect enhancements for anticancer drugs including paclitaxel (PTX) or doxorubicin (DOX), which might be promising for combating MDR1-mediated resistance. However, this PEGylated "nano" strategy to combat MDR1 mediated drug resistance remained largely unexplored.

Cyclodextrins (CDs), which are cyclic molecules made of oligosaccharides, could serve as host cavities to encapsulate many anticancer drugs with suitable sizes by molecular recognition.[33] Due to their aqueous solubility and low toxicity or immunity, CDs with supramolecular self-assembly ability have been utilized to improve the solubility or stability of various chemotherapeutics.[34] As a typical, β-CD, composed of 7 D(+)-glucose units by α-1,4-

linkages, as well as its derivatives could enhance the solubility of hydrophobic paclitaxel (PTX) by forming inclusion complex in a 1:1 PTX/β-CD molecular ratio.[35] Furthermore, doxorubicin (DOX), as another popular chemotherapeutics, could also form complex with β-CD derivatives in a 1:2 DOX/β-CD molecular ratio for enhanced stability and bioavailability, indicating the importance of CDs in pharmaceutics.[36] To be mentioned, CD based nanoformulations have showed advantages in drug resistance.[37] For example, Uekama *et al.* reported that β-CD derivatives could interact with the cellular membrane and inhibit P-glycoprotein's drug efflux activity.[38] We also designed a series of cationic β-CD-OEI (β-cyclodextrin-oligo(ethylene imine)) copolymers for drug and gene co-delivery in form of nanoparticles to overcome Bcl-2 mediated drug resistance.[6] More recently, CD based stimulus responsive carriers have attracted increasing interests due to their promising application for on-demand drug delivery.[39, 40] For example, Li *et al.* modified a β-CD star polymer by further conjugation of thermosensitive poly(N-isopropylacrylamide) (PNIPAAm) arms, which could form nanoparticulated β-CD/PTX inclusion complex at 37 °C and promote cellular uptake of encapsulated PTX.[41] However, their stability remained a concern by considering the hydrophobicity of PNIPAAm at body temperature and it was also worthy to explore the *in vivo* anti-cancer effect of these CD based thermoresponsive nanoparticles. For stability improvement, it is also worth mentioned that a series of thermos-responsive polymers with further conjugation of oligo-(ethylene glycol) (meth)acrylate (OEGA) was recently reported to exhibit enhanced stability as well as satisfactory biocompatibility, without disturbance of ionic strength, pH, chain length, or thermal transition hysteresis, indicating their potential applications in reliable stimulus responsive biomaterials.[42] However, currently, there are still few reports on designing on-demand drug delivery carriers by taking the advantage of β-CD and OEGA.

In this study, we constructed a temperature responsive PEGylated star polymer based on conjugation of β-CD core with thermosensitive poly(N-isopropylacrylamide) (PNIPAAm) and biocompatible poly(oligo(ethylene glycol) acrylate) (POEGA) arms. By taking the advantage of PEG induced drug efflux function impairment in drug resistant cancer cells as well as its contribution in stability increase, we hypnosis that this β-CD-*g*-(PNIPAAm-*b*-POEGA)$_x$ star copolymer could form biocompatible and stable supramolecular nanoparticles at body temperature which could facilitate endocytosis of anticancer drug and impair MDR1 related drug resistance, as shown in **Scheme 1**. In details, the resultant start polymer could retain excellent drug-loading capacity at temperature below lower critical solution temperature (LCST), thanks to the self-assembly between host CD cavity and guest drug molecule as well as the aqueous solubility of POEGA and PNIPAAm chains. Furthermore, the increase of environment temperature to body temperature (37 °C, above LCST) would lead to the formation drug-polymer complex nanoparticles, which facilitated cellular endocytosis and impaired the membrane pump mediated drug resistance in *in vitro* and *in vivo* studies. To the best of our knowledge, it serves as a pioneer report of utilizing PEGylated CD based star polymer, with temperature sensitive nanoparticle formation ability, to combat MDR1 mediated *in vitro* and *in vivo* cancer drug resistance.

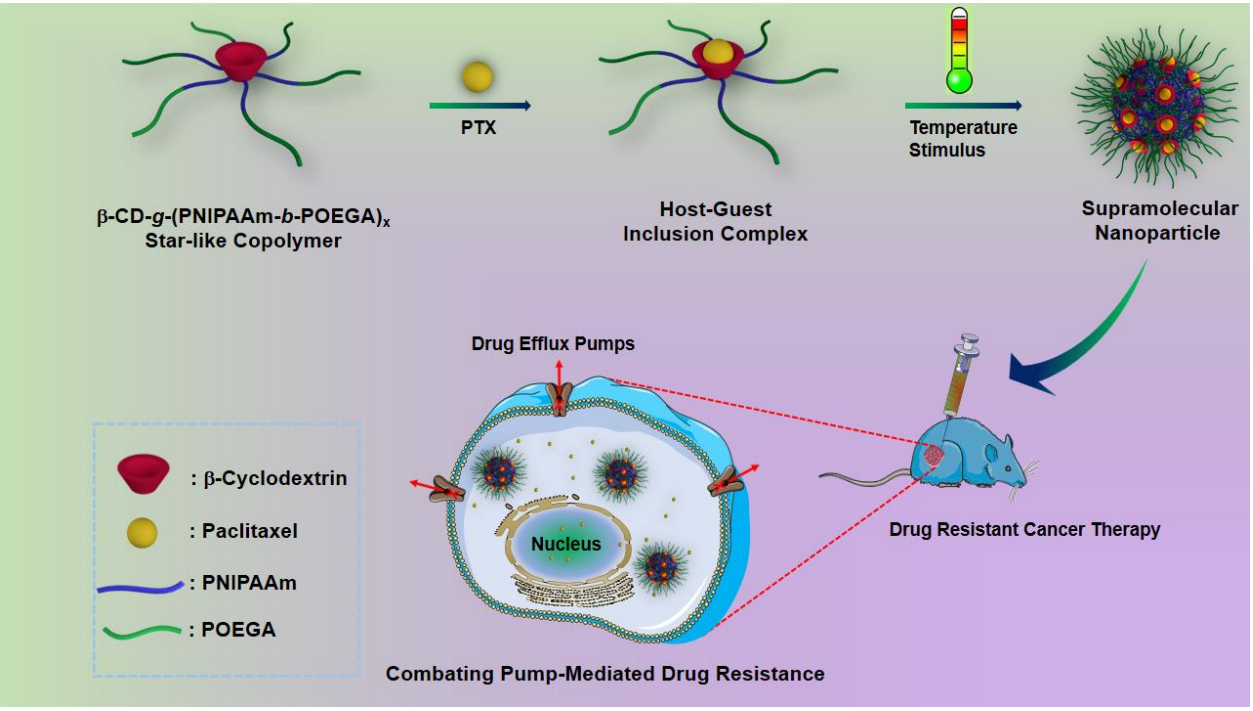

Scheme 1. Scheme illustration of star-like β-CD-*g*-(PNIPAAm-*b*-POEGA)$_x$ copolymer as well as its inclusion complex formation with chemotherapeutic PTX. The temperature induced supramolecular nanoparticle formation show enhanced endocytosis of PTX and increased intracellular retention by impairing the pump mediated drug resistance.

2. EXPERIMENTAL SECTION

2.1 Materials

β-Cyclodextrin (β-CD, Alladin) dried at 80 °C under reduced pressure overnight was utilized for further modification. Recrystallization for N-isopropylacrylamide (NIPAAm, Acros Organics) was conducted in n-hexane before use. Dioxane was dried by refluxing with the fresh sodium-benzophenone complex under N_2 and distilled before use. Dicyclohexylcarbodiimide

(DCC, Alladin, 97%) and 4-(dimethylamino) pyridine (DMAP, Alladin, 98%) were used as received. S-1-dodecyl-S′-(α, α'-dimethyl-α"-aceticacid) trithiocarbonae (DDAT) was utilized as chain transfer agent (CTA).[43, 44] Roswell Park Memorial Institute RPMI-1640 medium and Dulbecco's modified Eagles medium (DMEM) were supplied by Life Technology; TurboFect transfection reagent (Fermentas), SuperScript Reverse Transcriptase from Thermo Fisher Scientific; MDR1 antibody (22336-1-AP) was provided by Proteintech Technology; immuno-histochemistry detection reagent (8114S) from Cell Signaling Technology (CST); Poly(ethylene glycol) methyl ester acrylate, 2,2-Azoisobutyronitrile (AIBN), 4',6'-diamidino-2-phenylindole (DAPI), 3-(4,5-dimethythiazol-2-yl)-2,5-diphenyl tetrazolium bromide (MTT), paclitaxel (PTX), doxorubicin (DOX), puromycin, dimethylsulphoxide (DMSO) from Sigma-Aldrich; Trizol reagent, polymerase chain reaction (PCR) mixture regent and gel-red dye provided by Yeasen Biotech. The primers were synthesized by Sangon Biotech.

2.2 Synthesis of the reversible addition–fragmentation chain transfer (RAFT) macroinitiator β-CD-(CTA)$_x$

β-CD (1.040 g, 0.916 mmol; dried under vacuum at 80 °C overnight before use) and CTA (2.303 g, 6.414 mmol) were mixed in 30 mL anhydrous N,N-dimethylacetamide. After all the solid being dissolved completely, DCC (1.321g, 6.415 mmol) and trace amount of DMAP were added to initiate the β-CD modification of its –OH groups for 24 h reaction. The crude product was purified by cold diethyl ether precipitation and following centrifugation as well as vacuum dry, to collect a slight yellow powder.[45, 46]

2.3 Synthesis of multiple-arm star-like homogenous polymer β-CD-*g*-(PNIPAAm-CTA)$_x$ *via* RAFT polymerization

In a Schlenk flask, containing β-CD-(CTA)$_x$ (0.231 g, 0.073 mmol), NIPAAm (3.478 g, 0.031 mol) and AIBN (0.026 g, 0.001 mmol) within 25 mL anhydrous dioxane, nitrogen bubbling degassing was conducted for 20 min, before 7 h polymerization initiation at 70 °C in an oil bath. Crude product was precipitated in cold diethyl ether to remove unreacted monomer and further filtration as well as vacuum dry at 40 °C was performed. Proton nuclear magnetic resonance (NMR) and gel permeation chromatography (GPC) characterizations were used to obtain the averaged molecular weight (M_n) of final product as $M_{n,\,NMR}$ =15,390 g/mol and $M_{n,\,GPC}$ =16,540 g/mol, with M_w/M_n =1.70.

2.4 Synthesis of multiple-arm star-like copolymer β-CD-*g*-(PNIPAAm-*b*-POEGA)$_x$ *via* RAFT polymerization

Macroinitiator β-CD-*g*-(PNIPAAm-CTA)$_x$ (1.049 g, 0.068 mmol), OEGA (1.603 g, 3.340 mmol) and AIBN (0.007 g, 0.041 mmol) were added into a flask with 5 mL anhydrous dioxane. Subsequently, the solution was purged by nitrogen bubbling to remove oxygen with stirring, before 24 h polymerization in 70 °C oil bath. Similar to previous case, diethyl ether was used to precipitate the crude product before vacuum drying at 40 °C. The average molecular weight of final product was calculated to be $M_{n,\,NMR}$ =26,900 g/mol or $M_{n,\,GPC}$ =22,100 g/mol, with M_w/M_n =1.75.

2.5 Overexpression of MDR1 in HepG2 and H460 cancer cells

The full length of MDR1 was cloned to the XbaI/BamHI site of pCDH vector to produce lentiviral particles of MDR1, and the sequence of primers as listed. The forward primer: 5'- GCT CTA GAA TGG ATC TTG AAG GGG ACC GCA ATG-3', the reverse primer: 5'- CGG GAT CCT CAC TGG CG CT TTG TTC CAG CCT-3'. Overexpressed lentivirus particles of MDR1 were harvested after HEK293T transfection with MDR1 lentiviral plasmid, and then infected into HepG2 liver cancer and NIH-H460 lung cancer cells. After 72 h, the transfected cells were further cultured with 5 μg/mL puromycin in complete medium for 2-3 days to select MDR1 stably expressed cell lines. Western blotting for protein expressioin analysis and reverse transcription polymerase chain reaction (RT-PCR) for message ribonucleic acid (mRNA) amount analysis were conducted to verify availability of stable expression cell lines. The sequence of primers for RT-PCR were as follows: MDR1 (forward: 5'- CGA CAG GAG ATA GGC TGG TT -3'; reverse: 5'- AGA ACA GGA CTG ATG GCC AA -3'), GAPDH (forward: 5'-AGG TCG GAG TCA ACG GAT TT -3'; reverse: 5'- ATC TCG CTC CTG GAA GAT GG-3')

2.6 Supramolecular self-assembly between β-CD-*g*-(PNIPAAm-*b*-POEGA)$_x$ polymer and chemotherapeutics

The general process for fabricating host-guest complex of β-CD-*g*-(PNIPAAm-*b*-POEGA)$_x$/PTX or β-CD-*g*-(PNIPAAm-*b*-POEGA)$_x$/DOX was described as follows. Briefly, a solution of PTX or DOX (1 mg) in ethanol (2 mL) was respectively added to 5 mL aqueous solution of β-CD-*g*-(PNIPAAm-*b*-POEGA)$_x$ (10 mg), before 24 h stirring. After complex formation, crude product could be harvested and centrifuged to dislodge the insoluble compound,

while the solvent was lyophilized overnight by freeze drier. Then the final product was subjected to calculate the yield and complex formation efficiency by using nuclear magnetic resonance (NMR) characterizations.

2.7 Cell culture

HepG2 liver cancer cells and NIH-H460 lung cancer cell were supplied by American Type Culture Collection (ATCC). Both cells were cultured at 37 °C, 5% CO_2, DMEM or RPMI1640 culture medium supplemented with 10% fetal bovine serum (FBS). HepG2/MDR1, H460/MDR1 and the respective control were maintained with 1 μg/mL puromycin for stable selection.

2.8 Cell viability assay

Cell viability *in vitro* was quantified by using MTT assay. 5×10^3 MDR1-overexpression and the respective control cells per well were seeded onto 96 well culture plates, before 24 h treatments of various compounds. After that, 10 μL of MTT (50 μg) aqueous solution was added for 4 h treatment, which was followed by supernatent removal and crystal dissolution in DMSO. After 10 min shaking, 492 nm absorption was utilized to quantify the viable cells. The mean optical desity (OD) values were calculated and cell viability curves were obtained.

2.9 Western blotting

The protein from cell lysates were separated by using electrophoresis, before transfection to poly(vinylidene fluoride) (PVDF) membranes. After that, the MDR1 protein detection was achieved by primary antibody incubation and visualization by electrochemiluminescence (ECL) system.

2.10 Confocal assay

HepG2/MDR1 cells with density of 5000 cells per coverslip were seeded on glass coverslips, before treatments with β-CD-*g*-(PNIPAAm-*b*-POEGA)$_x$/DOX at 37 °C or 25 °C. After that, cells were fixated by 4% paraformaldehyde (PFA) treatment as well as Triton X-100 and glycine permeabilization. DAPI was utilized to stain intracellular nucleus and further imaged by using a Leica LSM-510 confocal microscope.

2.11 Flow cytometry analysis

The cellular uptake of DOX was analyzed by flow cytometry. About 4×10^5 HepG2/MDR1 cells were seeded in 6-wells plate. After 24 h incubation, the cells were treated with β-CD-*g*-(PNIPAAm-*b*-POEGA)$_x$/DOX@NPs and cultured at different culture temperature (at 37 °C or 25 °C) for 12 h or 24 h. And the cells were harvested by trypsin with 0.25 % EDTA, and washed three times with PBS, then the cells were filtrated by cell filter and examined by flow cytometer with detection wavelengths 488 nm. The number of the detected cells were over 1×10^4 for each sample.

2.12 *In vitro* drug release study

The β-CD-*g*-(PNIPAAm-*b*-POEGA)$_x$/DOX@NPs with 1 mg doxorubicin (DOX) were prepared and left to dialysis bag and transferred into 50 mL phosphate buffer (PBS) solution (0.01M, pH= 7.2), and incubated in a shaker bath at 100 rpm and 37 °C or 25 °C. At indicated time, 1 mL buffer was collected from the vial and replaced with fresh PBS buffer. The amount of released DOX was tested by detecting absorbance wavelengths at 480 nm with UV-Vis spectrophotometer.

2.13 Animal *in vivo* study

Nude mice (sparse fur, 17-19 g, 5-6 weeks old) were transplanted subcutaneously with 2×10^6 HepG2/MDR1 cells in 100 μL phosphate buffer saline solution. After 4 days of transplantation, mice were injected intratumorally once every two days with β-CD-*g*-(PNIPAAm-*b*-POEGA)$_x$/PTX (C_{PTX} = 5 mg/kg), Taxol only (PTX in the mixture of Cremophor EL (polyoxyl 35 castor oil) and ethanol (1:1, v/v) with stock concentrion of 6 mg/mL and further dilution in PBS to make final solution with C_{PTX} = 5 mg/kg) or vehicle control, with daily monitoring of tumor size and body weight. At the end of 10 d, mice were sacrificed. Tumor volumes were calculated using the equation: volume (cm^3) = width^2 (cm^2) × length (cm)/2. The animal experiment was performanced by following the guidance of Animal Care and Use Committee of Xiamen University.

2.12 Hematoxylin and eosin (HE) staining and immunohistochemistry staining

The tumors and other organ tissues were removed for histological analysis after sacrifice. Paraffin sections were cut by using CM1900 cryostat microtome (Leica) with the thickness of 5 μm before HE staining. Proliferating cell nuclear antigen (PCNA) expression amount was

detected with PCNA antibody, and the sections were co-stained with hematoxylin to visualize nuclear. The HE staining or PCNA expression in all sections were observed by Olympus biomicroscope.

2.13 Statistical analysis

At least 6 independent experiments were conducted to collect the data in form of mean ± standard deviation (SD). Statistical significant difference was evaluated by using Origin 8 with the aid of Student's t tests (two-tailed).

3. RESULTS AND DISCUSSION

3.1 Synthesis of multi-arm β-CD-*g*-(PNIPAAm-*b*-POEGA)$_x$ star copolymer

The synthetic route to a star shape copolymer β-CD-*g*-(PNIPAAm-*b*-POEGA)$_x$ consisting of a β-CD core and multiple PNIPAAm-*b*-POEGA block copolymer arms was depicted in **Scheme 2**. By using the multifunctional initiator β-CD-(CTA)$_x$, the star shape copolymer β-CD-*g*-(PNIPAAm-*b*-POEGA)$_x$ was obtained by two sequential reversible addition fragmentation chain-transfer polymerizations (RAFT) of the monomers NIPAAm and OEGA.

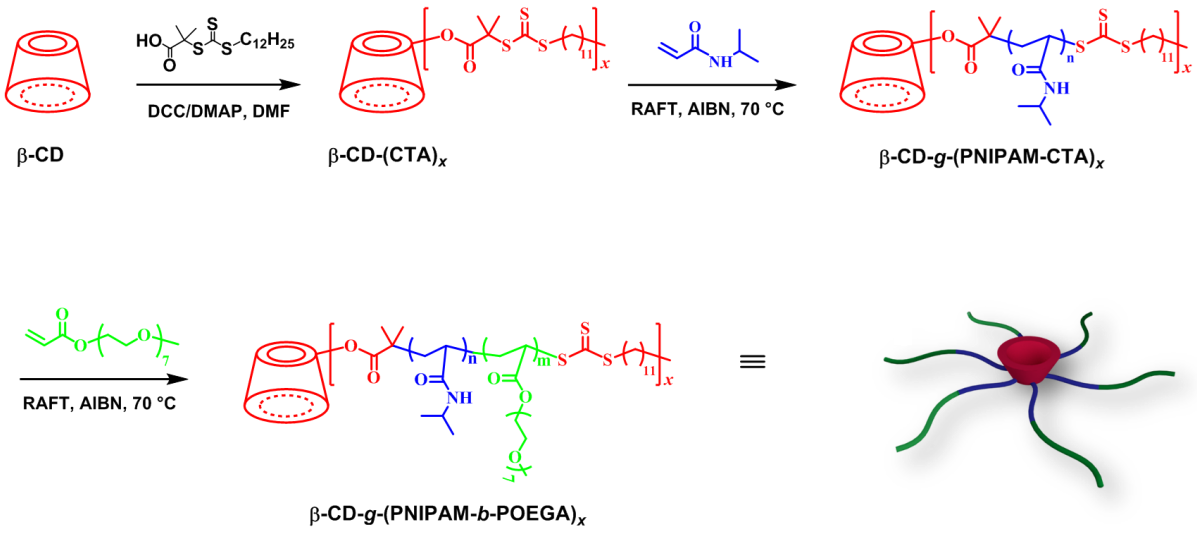

Scheme 2. Synthetic route and schematic illustration of temperature-responsive star-like β-CD-*g*-(PNIPAAm-*b*-POEGA)$_x$ host copolymer with POEGA in the distal arms.

The initiator β-CD-(CTA)$_x$ was simply synthesized by direct reaction of S-1-dodecyl- S′-(α,α′-dimethyl-α″-aceticacid) trithiocarbonate and β-CD in the presence of EDC and DMAP. The formed initiator had an average degree of substitution (DS) of 6, where the DS was defined as the number of CTA grafted on per CD molecule. The ^{1}H NMR spectrum of β-CD-(CTA)$_x$ was shown in **Figure 1**A, in which the signals corresponding to β-CD core and the grafted initiation groups CTA were observed clearly. The DS was calculated by the integration ratio of the signals for the methyl protons (a) at 1.72 ppm of the CTA group to those of the 1-postioned protons (-C(1)H) of β-CD at 4.85 ppm.

The as-prepared multifunctional initiator β-CD-(CTA)$_x$ initiated the RAFT polymerization of NIPAAm monomers to produce the multiple-arm star shape polymer β-CD-*g*-(PNIPAAm-CTA)$_x$. The ^{1}H NMR spectrum of the obtained polymer β-CD-*g*-(PNIPAAm-CTA)$_x$ was shown in Figure 1B, in which the characteristic signals (a, b, c, d, e) belonging to the PNIPAAm arms

could be clearly observed. The degree of polymerization (DP) of PNIPAAm arms was determined based on the integration ratio of signal (b') at 1.81 ppm to signal (d) at 4.01 ppm, which was 18.

Star shape host copolymer β-CD-*g*-(PNIPAAm-*b*-POEGA)$_x$ was further synthesized by sequential polymerization of OEGA monomers *via* RAFT and using β-CD-*g*-(PNIPAAm-CTA)$_x$ as initiator. Figure 1C showed the ^{1}H NMR spectrum of β-CD-*g*-(PNIPAAm-*b*-POEGA)$_x$, in which the new signals (f) and (g) could be assigned to the methylene protons (-C***H*$_2$**C***H*$_2$**O-) and end methyl protons (-OC***H*$_3$**) of OEGA, respectively. The DP of POEGA block was calculated through the integration ratio of signals (f) and (d), and the resultant value was 4. Based on these results, it could be concluded that the targeted star shape copolymer β-CD-*g*-(PNIPAAm-*b*-POEGA)$_x$ was successfully synthesized.

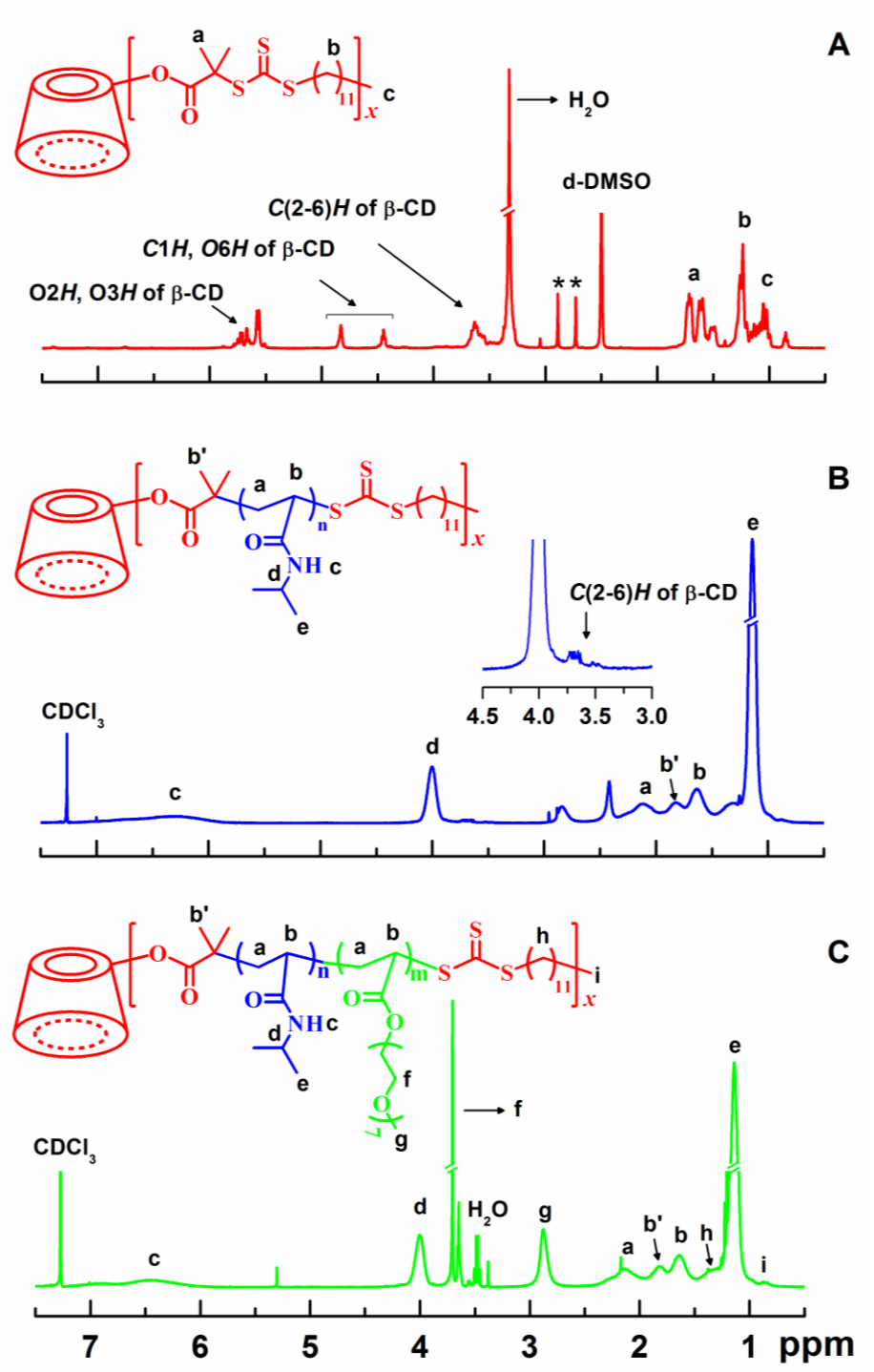

Figure 1. ^{1}H-NMR spectra of (A) β-CD-(CTA)$_x$ in d-DMSO; (B) β-CD-*g*-(PNIPAAm-CTA)$_x$ and (C) β-CD-g-(PNIPAAm-*b*-POEGA)$_x$ host copolymer in $CDCl_3$. The peak marked with * is attributed to the residual DMF present in the solvent.

3.2 Formation of supramolecular inclusion complex

The GPC trace of β-CD-*g*-(PNIPAAm-CTA)$_x$ was monomodal, indicating that β-CD-(CTA)$_x$ successfully initiated the polymerization of NIPAAm, as shown in **Figure 2**A, while the GPC trace of the obtained β-CD-*g*-(PNIPAAm-*b*-POEGA)$_x$ also exhibited the monomodal characteristic and shifted toward the higher molecular weight region as compared with its precursor, indicating the successful polymerization of OEGA monomers.[47-49] It is also worth mentioned that this β-CD-*g*-(PNIPAAm-*b*-POEGA)$_x$ star copolymer showed temperature responsive phase change, which was revealed by transmittance changes of β-CD-*g*-(PNIPAAm-*b*-POEGA)$_x$ solution with increasing temperatures.[45, 50, 51] As shown in Figure 2B, UV-vis (ultra violet – visible) spectrum was utilized to characterize the turbidity variation and showed that the lowest critical solution temperature (LCST) of β-CD-*g*-(PNIPAAm-*b*-POEGA)$_x$ was 36.4 °C. With temperature above LCST, the transmittance experienced a rapid decrease due to the phase change of PNIPAAm chain into hydrophobic status, which led to nanoparticulated aggregation in solution. By considering the nanoparticle facilitated cellular uptake, this temperature responsive behaviour might help thermoresponsive delivery of many pharmaceutics at body temperature (37 °C) above LCST.

Furthermore, aqueous β-CD-*g*-(PNIPAAm-*b*-POEGA)$_x$ star copolymer solution was mixed with paclitaxel (PTX) or doxorubicin (DOX) dissolved in ethanol at room temperature to allow the encapsulation of PTX or DOX guest molecules into β-CD host cavity by hydrophobic-hydrophobic interaction and size recognition. Successful inclusion complex formation between β-CD-*g*-(PNIPAAm-*b*-POEGA)$_x$ and PTX was confirmed by proton nuclear magnetic resonance (^{1}H NMR), as shown in Figure 2C. Due to the poor aqueous solubility of PTX, there was no

proton peaks observed from NMR spectrum by using D_2O as solvent. And the appearance of phenyl signals (δ 7.25-7.75) from β-CD-*g*-(PNIPAAm-*b*-POEGA)$_x$/PTX complex strongly provided the evidence of successful drug encapsulation. It could also be calculated that the ratio of β-CD-*g*-(PNIPAAm-*b*-POEGA)$_x$ to encapsulated PTX was 1:0.9, which indicated a 2.8 wt% drug loading amount and 90% encapsulation efficiency. Considering the negligible phenyl signals or low encapsulation rate of PTX when complexing with β-CD, Me-β-CD or HP-β-CD in previous reports,[41] the PEGylated β-CD-*g*-(PNIPAAm-*b*-POEGA)$_x$ with significantly improved solubilization of PTX might be due to its hydrophilic POEGA chains to promote inclusion complex formation. In the case of DOX, the complex formation was confirmed by fluorescence emission measurements of DOX as shown in Figure 2D. The fluorescence intensity of DOX at 600 nm was visualized to decrease to around 60% of original value, with addition of β-CD-*g*-(PNIPAAm-*b*-POEGA)$_x$, which was similar to previous report.[52]

The increase of stability by PEGylated β-CD-*g*-(PNIPAAm-*b*-POEGA)$_x$ was also confirmed by using hydrodynamic diameter measurements. Due to the thermo-responsive ability and phase transition of PNIPAAm chains, the resultant β-CD-*g*-(PNIPAAm-*b*-POEGA)$_x$ was expected to form aggregates at temperature above LCST. However, the previous report showed that the conjugation of PNIPAAm only to β-CD core might induce the formation of nanoparticles with size above 600 nm at body temperature.[41] Interestingly, as shown in Figure 2E-F by dynamic light scattering (DLS) and transmission electron microscopy (TEM), β-CD-*g*-(PNIPAAm-*b*-POEGA)$_x$ at 37 °C could form stable nanoparticles with PTX with average particle size of around 184 nm, while the formation of inclusion complex with DOX only increased the size a bit

to be 207 nm, which might favors the enhanced permeability and retention (EPR) effect in the size range of around 200 nm, indicating the advantage of incorporating POEGA chains.[53-55]

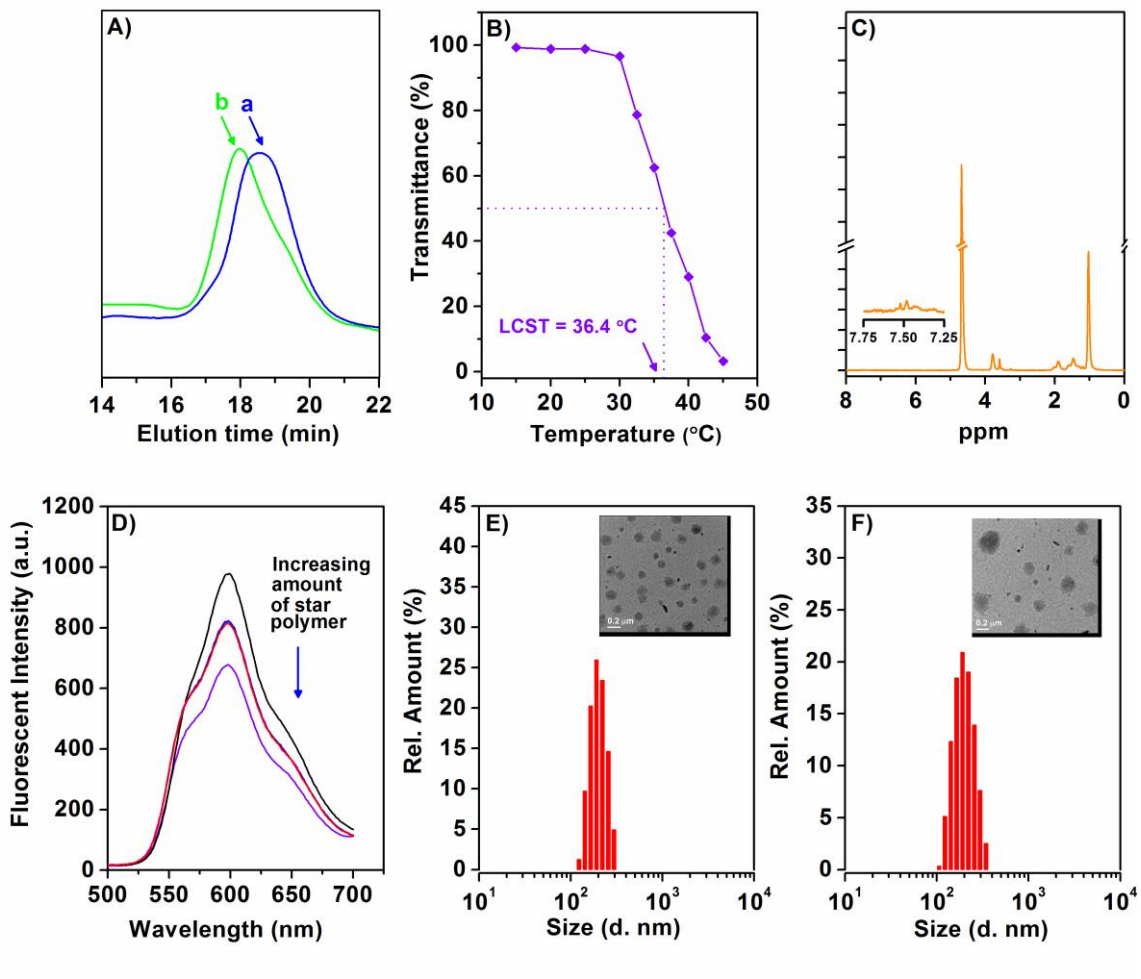

Figure 2. Characterizations of β-CD-*g*-(PNIPAAm-*b*-POEGA)$_x$ star-like copolymer and its supramolecular inclusion complex with chemotherapeutic drugs. (A) GPC traces of (a) β-CD-*g*-(PNIPAAm-CTA)$_x$ and (b) β-CD-*g*-(PNIPAAm-*b*-POEGA)$_x$ star-like copolymers. (B) Thermo-responsive behavior of β-CD-*g*-(PNIPAAm-*b*-POEGA)$_x$ star-like copolymer aqueous solutions as a function of temperature. Polymer concentration at 2.0 mg/mL was used in the measurement. (C) ^{1}H NMR spectra of β-CD-*g*-(PNIPAAm-*b*-POEGA)$_x$/PTX host-guest inclusion complex in

D_2O. (D) Fluorescence emission spectra of DOX in the presence of increasing amount of β-CD-*g*-(PNIPAAm-*b*-POEGA)$_x$ star polymer. Particle size distribution of (E) β-CD-*g*-(PNIPAAm-*b*-POEGA)$_x$/PTX and (F) β-CD-*g*-(PNIPAAm-*b*-POEGA)$_x$/DOX supramolecular nanoparticles at 37 °C. The inset graphs show the particle morphologies recorded by TEM (scale bar: 200 nm)

3.3 Construction of cancer cells with upregulated expression of MDR1

For the purpose of establishing MDR1 (P-glycoprotein) upregulated cell lines and verifying their drug resistance ability, lentivirus vectors carrying MDR1 gene were utilized for HepG2 liver cancer cell or H460 non-small lung cancer cell transfections. Puromycin screening was further conducted to obtain MDR1 stably upregulated cell lines (HepG2/MDR1 or H460/MDR1 cells), where their MDR1 mRNA levels or protein expressions were confirmed by RT-PCR or western blot respectively, shown in **Figure 3**A-B. Experimental results revealed that both MDR1 protein expression and mRNA level increases were achieved in HepG2/MDR1 or H460/MDR1 cell lines, indicating the successful establishment of MDR1 upregulated cancer cells.

Furthermore, in order to verify whether MDR1 high expression was sufficient for drug resistant phenotype, the viability of HepG2/MDR1 or H460/MDR1 cells was compared with HepG2-v or H460-v (the cell lines with vector only) with drug treatments to evaluate their tolerance of PTX or DOX, as shown in Figure 3C-F. It was worth mentioned that PTX with concentrations of 5–60 nM could lead to large cell death in HepG2-v or H460-v control cells but their effects on HepG2/MDR1 or H460/MDR1 cells were significantly reduced, as shown in Figure 3C-F. The half maximal inhibitory concentration (IC50) values for PTX increased from 6.6 nM in HepG2-v cells to 64.9 nM in HepG2/MDR1 cells or for DOX increased from 0.2 μM

in HepG2-v cells to 7.5 μM in HepG2/MDR1 cells. Similarly, the IC50 values for PTX were also promoted from 7.2 nM in H460-v cells to 49.3 nM in H460/MDR1 cells or for DOX from 0.2 μM in H460-v cells to 6.5 μM in H460/MDR1 cells, which confirmed the drug resistance increase in MDR1 upregulated cancer cells.

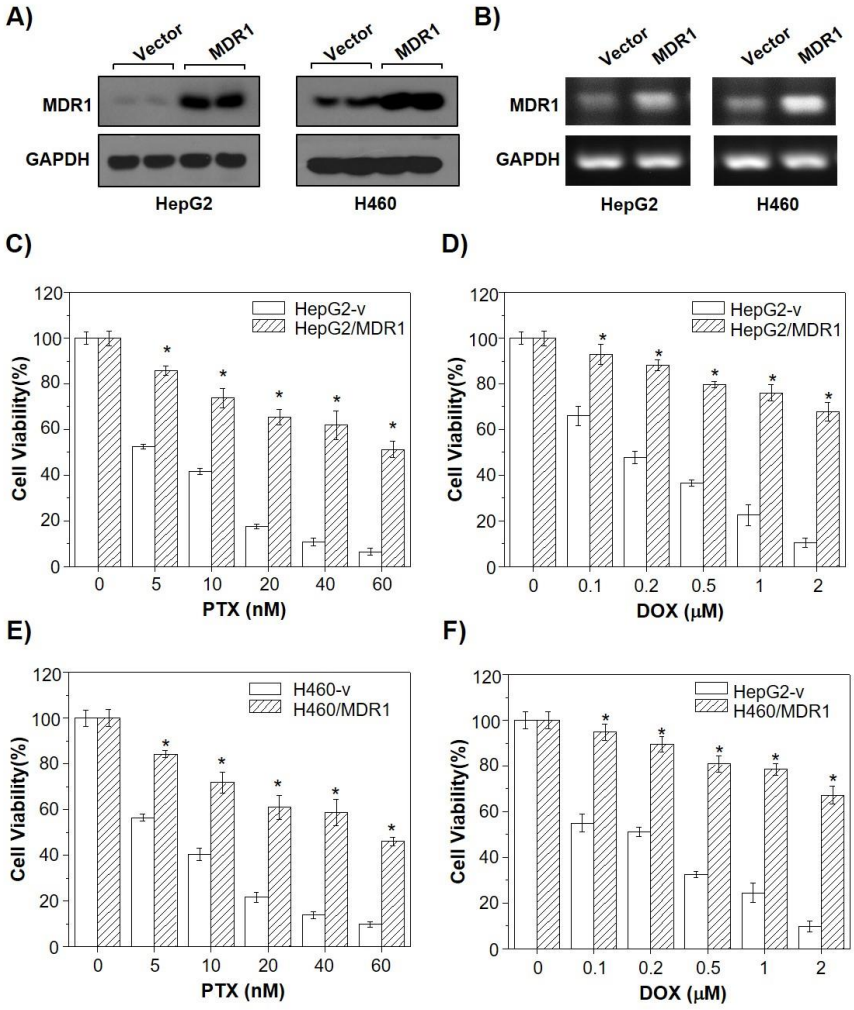

Figure 3. Establishment of drug resistant HepG2/MDR1 or H460/MDR1 cancer cell lines. (A) Western blotting to analyze the protein expression of MDR1 in MDR1-overexpressing or vector control HepG2 and H460 cells. (B) RT-PCR assay to examine the MDR1 mRNA expression in MDR1 overexpression HepG2/MDR1 and H460/MDR1 or vector control cell lines. (C-F) MTT

assay was conducted to detect the cell viability of HepG2/MDR1, H460/MDR1 and vector control cell lines in increasing dose of PTX or DOX. Data represents in the form of mean ± standard derivatives. *p < 0.05, compared with the vector control cell line respectively, n = 6.

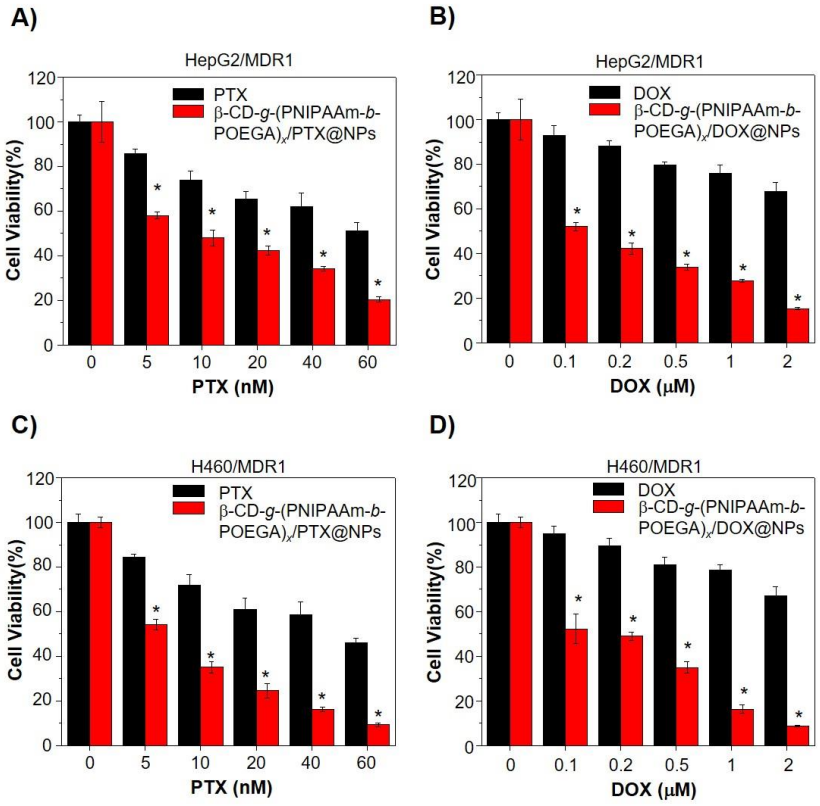

Figure 4. Cell viability assay to study β-CD-*g*-(PNIPAAm-*b*-POEGA)$_x$/drug complex nanoparticles for reversing MDR1-related drug resistance. (A) Cell viability of HepG2/MDR1 and (C) H460/MDR1 after 24 h treatment with indicated doses of PTX complex nanoparticles or equivalent PTX only. (B) Treatment with DOX complex nanoparticles or equivalent DOX only in HepG2/MDR1 and (D) H460/MDR1 cell lines for 24 h. Data represents in the form of mean ±

standard derivatives. *p < 0.05, with comparison to growth inhibition of PTX or DOX treatment only, n = 6.

Interestingly, above chemotherapeutic resistance could be reversed by drug delivery in form of nanoparticulated supramolecular inclusion complex of β-CD-*g*-(PNIPAAm-*b*-POEGA)$_x$/PTX@NPs or β-CD-*g*-(PNIPAAm-*b*-POEGA)$_x$/DOX@NPs, as shown in **Figure 4**. In details, the IC50 value for PTX was 64.9 nM in drug resistant HepG2/MDR1 liver cancer cells or 49.3 nM in drug resistant H460/MDR1 lung cancer cells respectively, while its IC50 value was reduced to be 11.8 nM in HepG2/MDR1 or 6.7 nM in H460/MDR1 cells in form of β-CD-*g*-(PNIPAAm-*b*-POEGA)$_x$/PTX@NPs complex nanoparticles. Similarly, the IC50 values of DOX were reduced from 7.5 μM in HepG2/MDR1 cells or 6.5 μM in H460/MDR1 cells to 0.1 μM in both cell lines, indicating the significant drug resistant cancer cell death rate increase by incorporating chemotherapeutics in rationally designed β-CD-*g*-(PNIPAAm-*b*-POEGA)$_x$ carrier.

3.4 Thermoresponsive cellular uptake of β-CD-*g*-(PNIPAAm-*b*-POEGA)$_x$/drug complex nanoparticles

In order to understand the possible of increased drug resistant cell growth inhibition by β-CD-*g*-(PNIPAAm-*b*-POEGA)$_x$/drug complex, fluorescent DOX was utilized as a model chemotherapeutic to study its *in vitro* cellular uptake, as shown in **Figure 5**. Experimental results showed that the cellular uptake of DOX was low due to the high expression of MDR1 proteins in HepG2/MDR1 cells. Similar case was observed for β-CD-*g*-(PNIPAAm-*b*-POEGA)$_x$/DOX

sample at 25 °C, a temperature below polymer's LCTS, within 24 h. Interestingly, much higher and faster cellular uptake of fluorescent DOX could be visualized at 37 °C or above LCST, thanks to the PNIPAAm phase change induced nanoparticle formation, as shown in Figure 5A-D. At temperature above LCST, PNIPAAm blocks could turn to be hydrophobic and their aggregation became the core of nanoparticles while the flexible POEGA chains maintained the stability of nanoparticles, which might greatly favour endocytosis mediated intracellular transportation of the inclusion complex nanoparticles as well as intracellular chemotherapeutics retention time increase. Furthermore, flow-cytometry quantitative analysis of cell counts with DOX fluorescent signals was also conducted to confirm the HepG2/MDR1 cell uptake of fluorescent DOX in form of β-CD-*g*-(PNIPAAm-*b*-POEGA)$_x$/DOX inclusion complex nanoparticles. As shown in Figure 5E, the DOX fluorescence intensity within HepG2/MDR1 cells increased with incubation temperature and time, which was similar to the observation of fluorescent images in Figure 5A-D. To further understand the effect of growth inhibition of β-CD-*g*-(PNIPAAm-*b*-POEGA)$_x$/drug complex at different temperature, the in *vitro* drug release of β-CD-*g*-(PNIPAAm-*b*-POEGA)$_x$/drug was performed at 37 °C (a temperature above polymer's LCST) or 25 °C (a temperature below polymer's LCST) for indicated time, as shown in Supporting Figure S1. Experimental results showed that β-CD-*g*-(PNIPAAm-*b*-POEGA)$_x$/DOX complex showed a thermoresponsive drug release profile. At 37 °C condition, DOX was promptly released from polymer complex in the first six hours, over 80 % drug was released, and the cumulative released drug was up to 90 % after 24 h culture. Whereas, once replacement of conditions at 25 °C, a slowly release of drug was observed during 24 h and the accumulated released drug was only 53.9 %, it was far less than released efficiency at 37 °C. In short, the

favorable cell uptake and drug release was achieved at 37 °C for β-CD-*g*-(PNIPAAm-*b*-POEGA)$_x$/DOX inclusion complex nanoparticles.

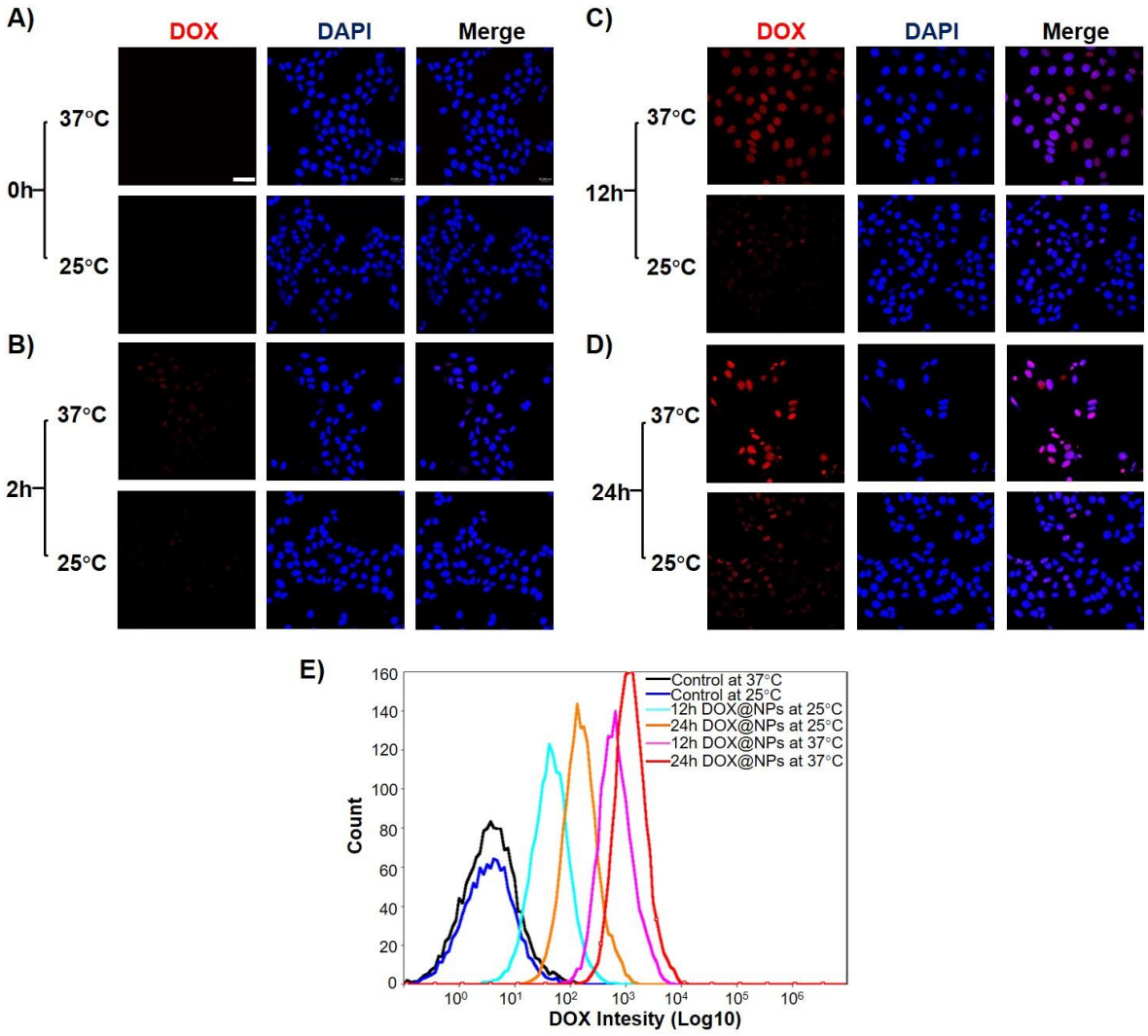

Figure 5. Thermo-responsive cellular uptake of β-CD-*g*-(PNIPAAm-*b*-POEGA)$_x$/DOX inclusion complex nanoparticles. (A-D) HepG2/MDR1 cells were plated in cover slip at previous day of treatment. Treatment with β-CD-*g*-(PNIPAAm-*b*-POEGA)$_x$ of the supramolecular complex was included with DOX at 37 °C and 25 °C for different time as indicated above. At end of the treatment, cells were fixed and examined by fluorescence microscopy. DAPI (blue)

was used to stain the cellular nuclei. The scale bar is 20 μm. (E) Flow cytometry measurements of HepG2/MDR1 cells with uptake of fluorescent DOX in form of β-CD-*g*-(PNIPAAm-*b*-POEGA)$_x$/DOX (DOX@NPs) at 37 °C and 25 °C for different time as indicated. Control sample indicated the behavior of the cells without any drug treatment.

3.5 Suprmolecular PEGylation could increase the stability of complex nanoparticle and enhanced cellular uptake in MDR-1 overexpressing cancer cells

Li *et al.* reported that β-CD baesd poly(N-isopropylacrylamide) (PNIPAAm) star polymer could form nanoparticulated β-CD-PNIPAAm/PTX inclusion complex at 37 °C and promote cellular uptake of encapsulated PTX.[41] However, this star polymer's stability remained a concern regarding the hydrophobicity of PNIPAAm at 37 °C. As shown in Figure 6A, β-CD-*g*-(PNIPAAm)$_x$ nanoparticles as well as β-CD-*g*-(PNIPAAm)$_x$/PTX or β-CD-*g*-(PNIPAAm)$_x$/DOX inclusion complex nanoparticles experienced fast size broadening at physiological salt condition (150 mM) within 30 min. Interestingly, with PEGylation, β-CD-*g*-(PNIPAAm-*b*-POEGA)$_x$ nanoparticles as well as β-CD-*g*-(PNIPAAm-*b*-POEGA)$_x$/PTX or β-CD-*g*-(PNIPAAm-*b*-POEGA)$_x$/DOX inclusion complex nanoparticles were quite stale with monomodal size distribution and average hydrodynamic size around 200 nm, even at physiological salt condition as shown in Figure 6B, indicating the importance of POEGA chains in preventing particle aggregation. More importantly, the experimental results also revealed that this stability increased also benefit the cellular uptake of inclusion complex nanoparticles in MDR-1 overexpressing HepG2 liver cancer cells. As shown in Figure 6D, the cellular uptake of β-CD-*g*-(PNIPAAm-*b*-POEGA)$_x$/DOX inclusion complex nanoparticles with PEGylation was significantly improved in

comparison with β-CD-*g*-(PNIPAAm)$_x$/DOX nanoparticles without PEGylation in Figure 6C, within 12 h or 24 h. This may be due to the fact that the size instability hindered the cellular uptake of non-PEGylated nanoparticles with aggregation and larger size. In short, the PEGylation served a key role in the design of supramolecular nanocomplex in terms of stability increase and favorable cellular uptake, which were important for their *in vitro* or *in vivo* drug delivery.[56-59]

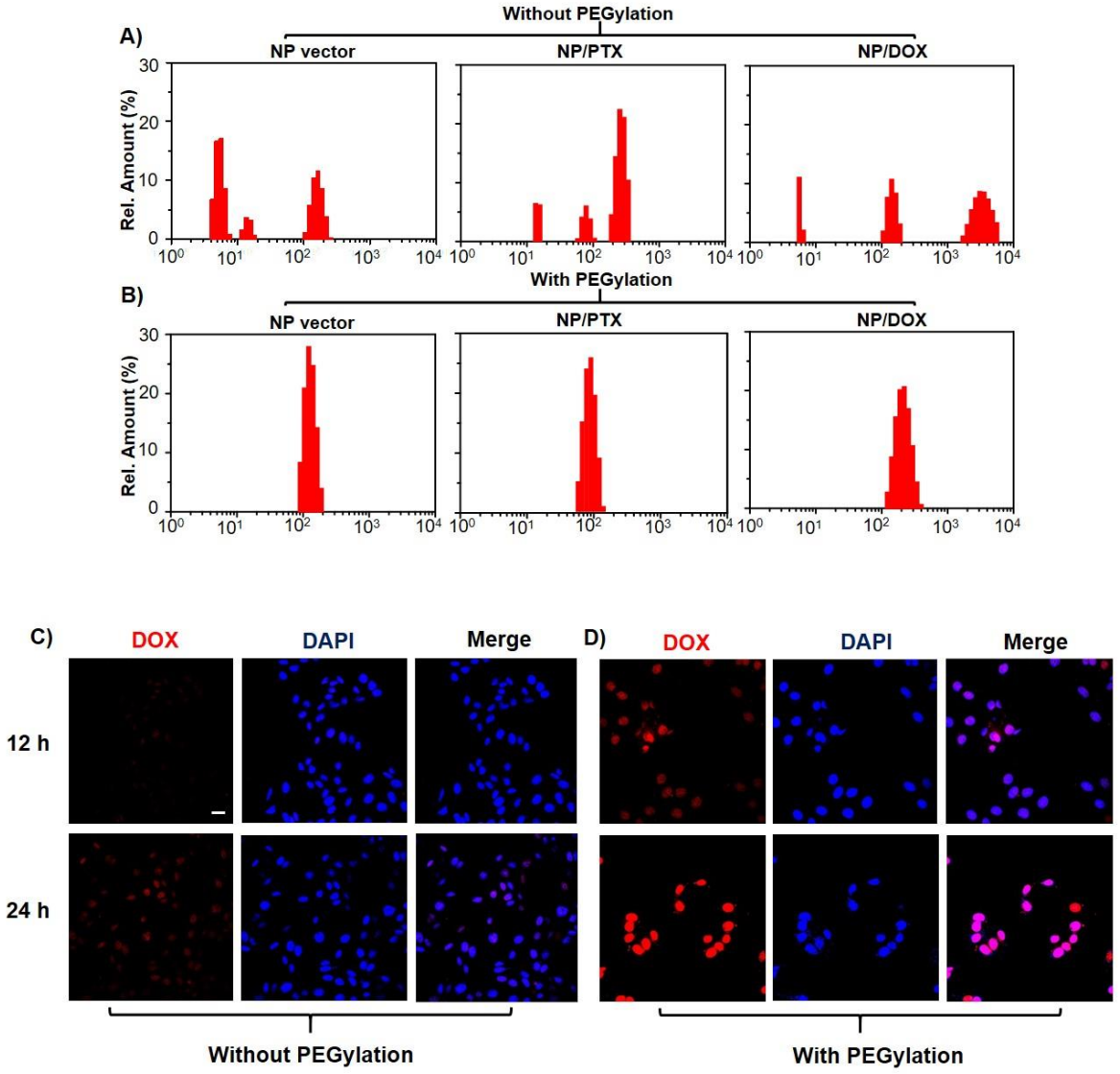

Figure 6. (A-B) Hydrodynamic size measurements of unPEGylated β-CD-*g*-$(PNIPAAm)_x$ or PEGylated β-CD-*g*-$(PNIPAAm\text{-}b\text{-}POEGA)_x$ nanoparticles without or with inclusion complex with PTX or DOX in 150 mM phosphate buffered saline (PBS) for 30 min. (C-D) Fluorescent imaging of cellular uptake of unPEGylated β-CD-*g*-$(PNIPAAm)_x$/DOX or PEGylated β-CD-*g*-$(PNIPAAm\text{-}b\text{-}POEGA)_x$/DOX nanoparticles in HepG2/MDR-1 cancer cells. DAPI (blue) was used to stain the cellular nuclei and DOX was shown in red. Scale bar = 25 μm.

3.6 *In vitro* MDR1 drug resistant cancer cell growth inhibition by temperature sensitive β-CD-*g*-$(PNIPAAm\text{-}b\text{-}POEGA)_x$/drug complex nanoparticles

To further verify whether the drug uptake and intracellular retention time increase could lead to improved growth inhibition of drug resistant HepG2/MDR1 cancer cells. *In vitro* cytotoxicity of HepG2/MDR1 or H460/MDR1 cancer cells with treatment of β-CD-*g*-$(PNIPAAm\text{-}b\text{-}POEGA)_x$ as well as its drug complex was tested based on MTT assay at 25 °C or 37 °C, as shown in **Figure 7**. As shown in Figure 7 and Supporting Figure S2, the host polymer β-CD-*g*-$(PNIPAAm\text{-}b\text{-}POEGA)_x$ showed very low cytotoxicity at both cancer cells with or without high expression of MDR1 proteins, indicating their biocompatibility. However, as shown in Figure 7 and Supporting Figure S3, the HepG2/MDR1 or H460/MDR1 cell growth was significantly inhibited with treatment of β-CD-*g*-$(PNIPAAm\text{-}b\text{-}POEGA)_x$/drug complex at 37 °C rather than at 25 °C, indicating the importance of thermo-responsive properties of this star polymeric carrier.

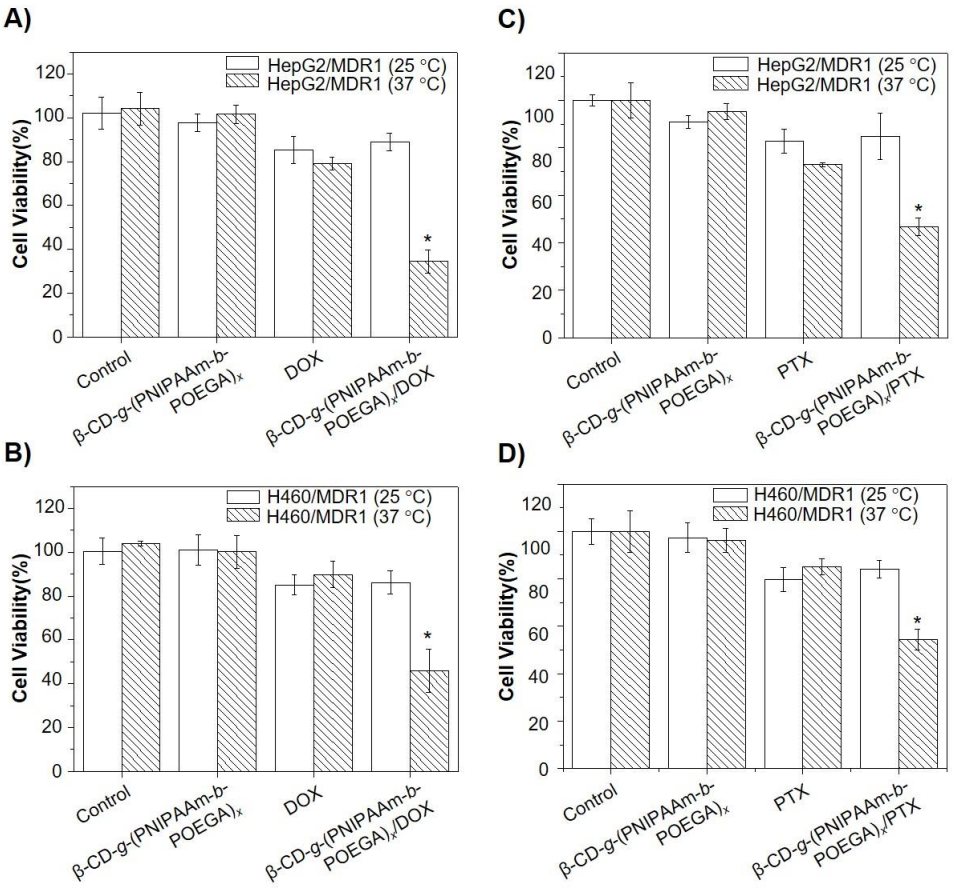

Figure 7. *In vitro* MDR1 drug resistant cancer cell growth inhibition by temperature sensitive β-CD-*g*-(PNIPAAm-*b*-POEGA)$_x$/drug complex. (A-B) Cell viability measured by MTT in (A) HepG2/MDR1 or HepG2 vector control cells and (B) H460/MDR1 or H460 vector control cells with treatments of β-CD-*g*-(PNIPAAm-*b*-POEGA)$_x$, DOX (0.5 μM) and β-CD-*g*-(PNIPAAm-*b*-POEGA)$_x$/DOX inclusion complex at 37 °C or 25 °C for 24 h. (C-D) Drug resistant cancer cell growth inhibition by PTX (10 nM) as well as its complex form of β-CD-*g*-(PNIPAAm-*b*-POEGA)$_x$/PTX in (C) HepG2/MDR1 or (D) H460/MDR1 cells at different environmental temperatures. Data represents in the form of mean ± standard derivatives. *$p < 0.05$ was considered as significant difference in comparison with the cell viability at 25 °C, n = 6.

3.7 *In vivo* study of drug delivery by thermo-sensitive β-CD-*g*-(PNIPAAm-*b*-POEGA)$_x$@NPs for potential drug resistant cancer therapy

To further investigate whether PTX delivery in form of β-CD-*g*-(PNIPAAm-*b*-POEGA)$_x$/PTX@NPs could improve its therapeutic effect, *in vivo* HepG2/MDR1 tumor xenograft nude mice model was established in **Figure 8**. Experimental results showed that, compared with Taxol treatment only, β-CD-*g*-(PNIPAAm-*b*-POEGA)$_x$/PTX@NPs complex nanoparticles with PTX encapsulation ability could greatly hinder HepG2/MDR1 tumor growth. In details, as shown in Figure 8A-C, the control tumor with saline treatment only increased its size from 73 mm^3 ± 17 mm^3 to 1552 mm^3 ± 584 mm^3 in 10 d experiment, indicating a significant tumor size increase without any chemotherapy. It was worth mentioned that, even with Taxol (PTX formulation in currently commercial formulation of Cremophor EL and ethanol) treatment, HepG2/MDR1 tumor still increased its size to be 1242 mm^3 ± 727 mm^3, indicating that Taxol only was not sufficient to inhibit HepG2/MDR1 tumor growth which was similar to *in vitro* cellular experimental results in Figure 3, because of its *in vivo* drug resistance. However, this drug resistant tumor was observed to reach its final volume of 157 mm^3 ± 68 mm^3 with treatment of β-CD-*g*-(PNIPAAm-*b*-POEGA)$_x$/PTX@NPs, which might be due to the successful enhanced retention of intracellular PTX after formation of supramolecular inclusion complex nanoparticles.

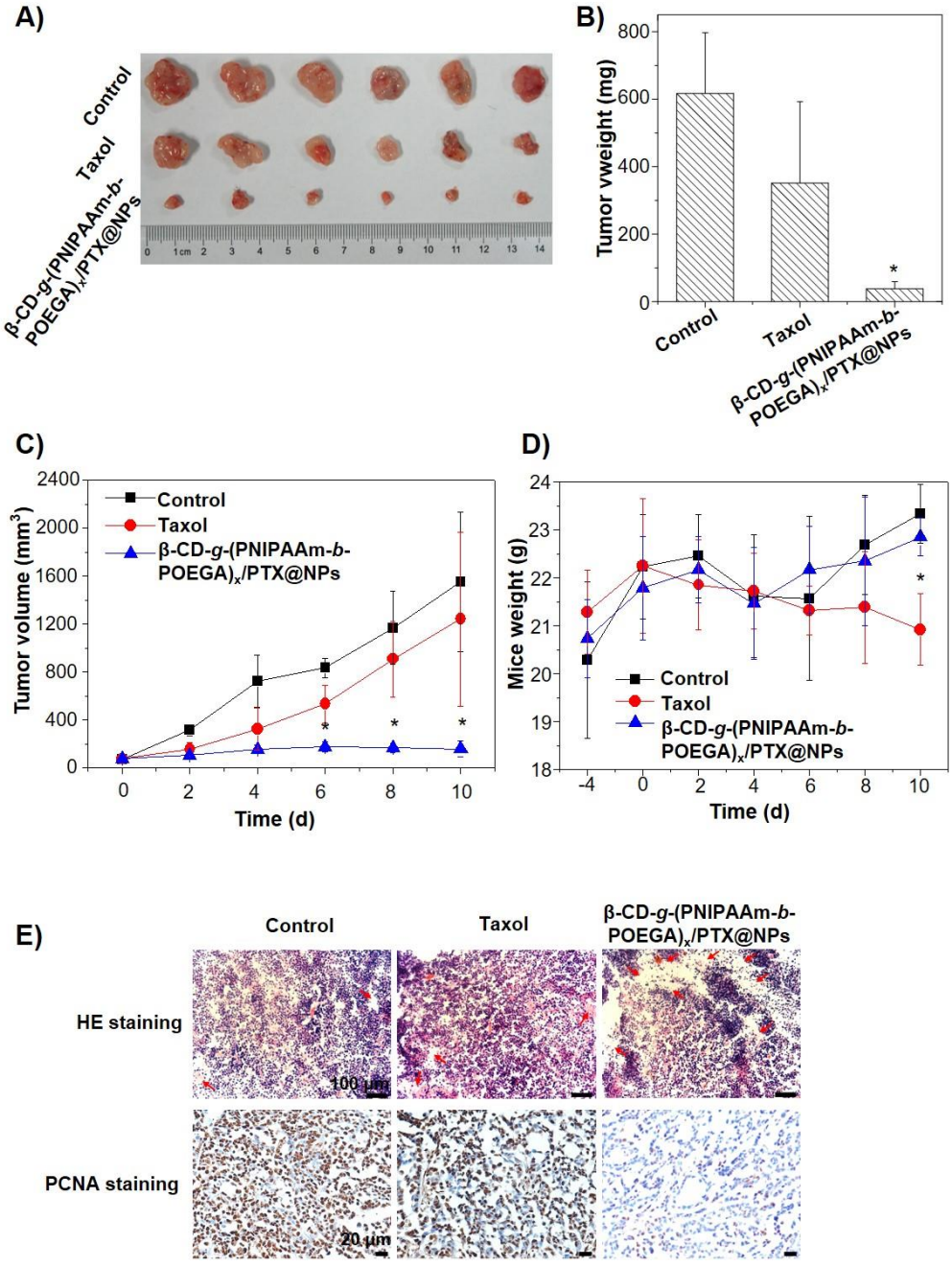

Figure 8. *In vivo* study of drug delivery by thermosensitive β-CD-*g*-(PNIPAAm-*b*-POEGA)$_x$ nanoparticles for potential drug resistant cancer therapy. (A) Tumor images of HepG2/MDR1 xenograft and (B) tumor weight were calculated with the treatment of β-CD-*g*-(PNIPAAm-*b*-POEGA)$_x$/PTX inclusion complex drug or PTX in the formulation of Taxol only after 10 days.

(C) Indicate a significant reduction in tumor volume between Taxol-treated group and β-CD-*g*-(PNIPAAm-*b*-POEGA)$_x$ inclusion PTX complex. (D) The mice weight changes with different treatments. (E) Paraffin-embedded sections were subjected to immunohistochemical analysis with hematoxylin and eosin (HE) staining and proliferating cell nuclear antigen (PCNA) expression after indicated treatment for 10 days. Data represents in the form of mean ± standard derivatives. *$p<0.05$, in comparison with treatment of Taxol only, $n = 6$.

Similar to tumor size increase inhibition, tumor weight in β-CD-*g*-(PNIPAAm-*b*-POEGA)$_x$/PTX@NPs group was also observed to decrease to be about 30% of that in saline or Taxol only control groups (Figure 8B), without obvious side effects on the main organs or body weight of mice (Figure 9C & Figure 8D). At the end of experiments, solid tumors in sacrificed mice were separated for HE staining and proliferating cell nuclear antigen (PCNA) protein expression analysis (Figure 8E). HE staining results of representative tissue sections clearly exhibited an increase of necrotic or apoptotic areas in β-CD-*g*-(PNIPAAm-*b*-POEGA)$_x$/PTX@NPs group as indicated in red arrows, while this phenomenon was not obvious in saline or Taxol only control groups, indicating the therapeutic effect improvements due to the enhanced cellular uptake or intracellular retention of chemotherapeutics Furthermore, we also observed a few unexpected lesion spots in the HE staining of liver section for mice with Taxol treatment in Figure 9A-B, which was similar to previously reports.[60, 61] In clinical experiment, the toxicities with the administration of Taxol was largely reported in cases of serious inflammatory response, hypersensitivity reactions, or toxic effects of the blood system, cardiotoxicity, due to the application of excipient, cremophor EL (a polyoxyethylated castor oil), which might increase the risk of adverse reactions in PTX therapy.[62-64] It was worth mentioned that PTX in the polymeric nanoparticle formulation (PNIPAAm-*b*-POEGA)$_x$/PTX@NPs was not

able to induce this side effect as shown in Figure 9A-B, indicating that the solvent induced side effect in Taxol was not obvious in the formulation of drug-nanoparticles. More importantly, immunostaining of tissue sections showed that the administration of β-CD-*g*-(PNIPAAm-*b*-POEGA)$_x$/PTX@NPs lead to decreased expression of PCNA protein, an important cell proliferation marker,[65, 66] indicating the significant growth inhibition efficiency increase by PTX delivery in form of temperature sensitive β-CD-*g*-(PNIPAAm-*b*-POEGA)$_x$/PTX@NPs supramolecular inclusion complex nanoparticles. In short, PEGylated β-CD-*g*-(PNIPAAm-*b*-POEGA)$_x$ star polymer, with the ability to serve as a host molecule to encapsulate anticancer drugs by supramolecular self-assembly and to form stable nanoparticles at body temperature, was able to increase the therapeutic efficiency of chemotherapeutics even in *in vivo* drug resistant tumor model, indicating their promising applications in personalized cancer therapy.

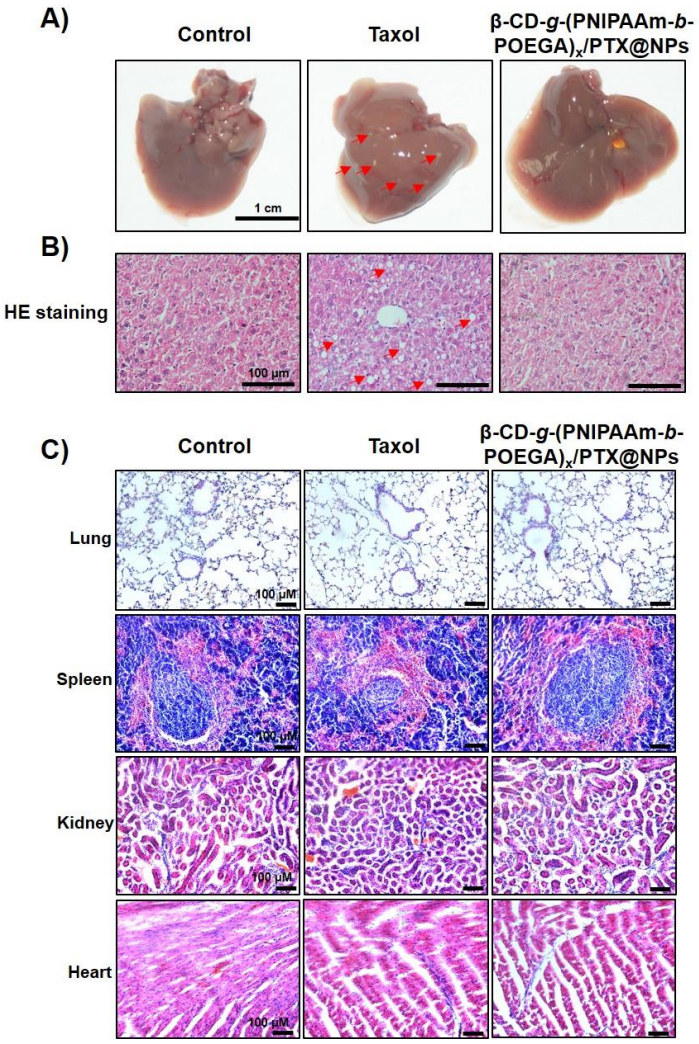

Figure 9. *In vivo* study of drug delivery by thermosensitive β-CD-*g*-(PNIPAAm-*b*-POEGA)$_x$ for potential drug resistant cancer therapy. The optical images (A) and HE staining (B) of liver in the mice with treatments of β-CD-*g*-(PNIPAAm-*b*-POEGA)$_x$/PTX@NPs, Taxol only, or saline control after 10 days. (C) Main organs including heart, spleen, lung, kidney of mice, with after β-CD-*g*-(PNIPAAm-*b*-POEGA)$_x$/PTX@NPs, Taxol only, or saline treatments, were sectioned and subjected to HE staining after 10 days.

4. Conclusion

In conclusion, a novel PEGylated β-CD-*g*-(PNIPAAm-*b*-POEGA)$_x$ star polymer with thermo-responsive property was designed to form a hierarchically self-assembled host-guest supramolecular structure with guest chemotherapeutic PTX or DOX embedded within the host β-CD cavity for better encapsulation. More importantly, this PEGylated star polymer could form stable nanoparticles at body temperature which favored cellular uptake and intracellular drug retention, resulting in impairing MDR1 mediated drug resistance. In addition, both *in vitro* and *in vivo* results revealed that drug resistance were greatly conquered by β-CD-*g*-(PNIPAAm-*b*-POEGA)$_x$/PTX@NPs in its nanoparticle form. All these positive results show high potential of using thermo-sensitive supramolecular nanocarrier strategy in drug resistant tumor therapy and personalized nanomedicine.

Supporting Information. Supplementary information includes the biocompatibility of β-CD-*g*-(PNIPAAm-*b*-POEGA)$_x$, and drug resistant cancer cell growth inhibition by temperature sensitive β-CD-*g*-(PNIPAAm-*b*-POEGA)$_x$/drug complex nanoparticles. Supplementary information accompanies this paper is available free of charge *via* the Internet at http://pubs.acs.org.

Acknowledgments

The authors would like to thank the supported by the National Natural Science Foundation of China (81773661, 21303145) and Fundamental Research Funds for the Central Universities (20720170066), and express gratitude to the A*STAR Research Grant for support of this project.

Notes

The authors declare no competing financial interests.

5. References

1. Beretta, G. L.; Cavalieri, F., Engineering Nanomedicines to Overcome Multidrug Resistance in Cancer Therapy. *Curr Med Chem* **2016,** 23, (1), 3-22.
2. Gottesman, M. M.; Fojo, T.; Bates, S. E., Multidrug resistance in cancer: role of ATP-dependent transporters. *Nat Rev Cancer* **2002,** 2, (1), 48-58.
3. Liu, Y.; Li, Q.; Zhou, L.; Xie, N.; Nice, E. C.; Zhang, H.; Huang, C.; Lei, Y., Cancer drug resistance: redox resetting renders a way. *Oncotarget* **2016,** 7, (27), 42740-42761.
4. Holohan, C.; Van Schaeybroeck, S.; Longley, D. B.; Johnston, P. G., Cancer drug resistance: an evolving paradigm. *Nat Rev Cancer* **2013,** 13, (10), 714-26.
5. Yu, C.; Zhou, M.; Zhang, X.; Wei, W.; Chen, X.; Zhang, X., Smart doxorubicin nanoparticles with high drug payload for enhanced chemotherapy against drug resistance and cancer diagnosis. *Nanoscale* **2015,** 7, (13), 5683-90.
6. Chen, X.; Qiu, Y.-K.; Owh, C.; Loh, X. J.; Wu, Y.-L., Supramolecular cyclodextrin nanocarriers for chemo- and gene therapy towards the effective treatment of drug resistant cancers. *Nanoscale* **2016,** 8, (45), 18876-18881.
7. Wu, Y. L.; Wang, H.; Qiu, Y. K.; Liow, S. S.; Li, Z.; Loh, X. J., PHB‐Based Gels as Delivery Agents of Chemotherapeutics for the Effective Shrinkage of Tumors. *Adv. Healthcare Mater.* **2016,** 5, (20), 2679-2685.
8. Wu, Y.-L.; Wang, H.; Qiu, Y.-K.; Loh, X. J., PLA-based thermogel for the sustained delivery of chemotherapeutics in a mouse model of hepatocellular carcinoma. *RSC Adv.* **2016,** 6, (50), 44506-44513.
9. Cai, P.; Leow, W. R.; Wang, X.; Wu, Y.-L.; Chen, X., Programmable Nano–Bio Interfaces for Functional Biointegrated Devices. *Adv. Mater.* **2017,** 29, 1605529.

10. Erkoc, P.; Cingöz, A.; Bagci-Onder, T.; Kizilel, S., Quinacrine Mediated Sensitization of Glioblastoma (GBM) Cells to TRAIL through MMP-Sensitive PEG Hydrogel Carriers. *Macromol. Biosci.* **2017,** 17, (2), 1600267.

11. Liu, X.; Chen, X.; Chua, M. X.; Li, Z.; Loh, X. J.; Wu, Y.-L., Injectable Supramolecular Hydrogels as Delivery Agents of Bcl-2 Conversion Gene for the Effective Shrinkage of Therapeutic Resistance Tumors. *Adv. Healthcare Mater.* **2017,** 6, (11), 1700159.

12. Li, Z.; Liu, X.; Chen, X.; Chua, M. X.; Wu, Y.-L., Targeted delivery of Bcl-2 conversion gene by MPEG-PCL-PEI-FA cationic copolymer to combat therapeutic resistant cancer. *Mater. Sci. Eng. C* **2017,** 76, 66–72.

13. Battistella, C.; Klok, H.-A., Reversion of P-gp-Mediated Drug Resistance in Ovarian Carcinoma Cells with PHPMA-Zosuquidar Conjugates. *Biomacromolecules* **2017,** 18, (6), 1855-1865.

14. Roy, A.; Zhao, Y.; Yang, Y.; Szeitz, A.; Klassen, T.; Li, S. D., Selective targeting and therapy of metastatic and multidrug resistant tumors using a long circulating podophyllotoxin nanoparticle. *Biomaterials* **2017,** 137, 11-22.

15. Trapani, A.; Palazzo, C.; Contino, M.; Perrone, M. G.; Cioffi, N.; Ditaranto, N.; Colabufo, N. A.; Conese, M.; Trapani, G.; Puglisi, G., Mucoadhesive Properties and Interaction with P-Glycoprotein (P-gp) of Thiolated-Chitosans and -Glycol Chitosans and Corresponding Parent Polymers: A Comparative Study. *Biomacromolecules* **2014,** 15, (3), 882-93.

16. Liu, Y.; Chiu, G. N., Dual-functionalized PAMAM dendrimers with improved P-glycoprotein inhibition and tight junction modulating effect. *Biomacromolecules* **2013,** 14, (12), 4226-35.

17. Yim, H.; Na, K., Polycationic Nanodrug Covered with Hyaluronic Acid for Treatment of P-Glycoprotein Overexpressing Cancer Cells. *Biomacromolecules* **2010,** 11, (9), 2387.

18. Zhang, Q.; Li, F., Combating P-glycoprotein-mediated multidrug resistance using therapeutic nanoparticles. *Curr. Pharm. Des.* **2013,** 19, (37), 6655.

19. Peng, M.; Kokuryo, D.; Cabral, H.; Wu, H.; Terada, Y.; Saga, T.; Aoki, I.; Nishiyama, N.; Kataoka, K., A pH-activatable nanoparticle with signal-amplification capabilities for non-invasive imaging of tumour malignancy. *Nat. Nanotechnol.* **2016,** 11, (8), 724.

20. Mura, S.; Nicolas, J.; Couvreur, P., Stimuli-responsive nanocarriers for drug delivery. *Nat. Mater.* **2013,** 12, (11), 991-1003.

21. Wu, Y.-L.; Engl, W.; Hu, B.; Cai, P.; Leow, W. R.; Tan, N. S.; Lim, C. T.; Chen, X., Nanomechanically Visualizing Drug–Cell Interaction at the Early Stage of Chemotherapy. *ACS Nano* **2017,** 11, (7), 6996-7005.

22. Cai, P.; Layani, M.; Leow, W. R.; Amini, S.; Liu, Z.; Qi, D.; Hu, B.; Wu, Y. L.; Miserez, A.; Magdassi, S.; Chen, X., Bio-Inspired Mechanotactic Hybrids for Orchestrating Traction-Mediated Epithelial Migration. *Adv. Mater.* **2016,** 28, (16), 3102-10.

23. Dan, Z.; Cao, H.; He, X.; Zhang, Z.; Zou, L.; Zeng, L.; Xu, Y.; Yin, Q.; Xu, M.; Zhong, D.; Yu, H.; Shen, Q.; Zhang, P.; Li, Y., A pH-Responsive Host-guest Nanosystem Loading Succinobucol Suppresses Lung Metastasis of Breast Cancer. *Theranostics.* **2016,** 6, (3), 435-445.

24. Hatziagapiou, K.; Bethanis, K.; Lambrou, G. I.; Yannakopoulou, K.; Karpusas, M.; Braoudaki, M.; Christoforides, E.; Tsorteki, F.; Milionis, V.; Kavantzas, N., Enhanced Gefitinib Cytotoxicity in the Presence of Cyclodextrins: In-Vitro and Biophysical Studies Towards Potential Therapeutic Interventions for Cancer. *J. Biomed. Nanotechnol.* **2017,** 13, (5), 522-533.

25. Liu, Y.; Pu, Y.; Sun, L.; Yao, H.; Zhao, B.; Zhang, R.; Zhang, Y., Folic Acid Functionalized γ-Cyclodextrin C60, A Novel Vehicle for Tumor-Targeted Drug Delivery. *J. Biomed. Nanotechnol.* **2016,** 12, (7), 1393-1403.

26. Gigliotti, C. L.; Minelli, R.; Cavalli, R.; Occhipinti, S.; Barrera, G.; Pizzimenti, S.; Cappellano, G.; Boggio, E.; Conti, L.; Fantozzi, R., In Vitro and In Vivo Therapeutic Evaluation of Camptothecin-Encapsulated β-Cyclodextrin Nanosponges in Prostate Cancer. *J. Biomed. Nanotechnol.* **2016,** 12, (1), 114.

27. Pei, Q.; Hu, X.; Wang, L.; Liu, S.; Jing, X.; Xie, Z., Cyclodextrin/Paclitaxel Dimer Assembling Vesicles: Reversible Morphology Transition and Cargo Delivery. *ACS Appl. Mater. Interfaces* **2017,** 9, (32), 26740-26748.

28. Lv, L.; Qiu, K.; Yu, X.; Chen, C.; Qin, F.; Shi, Y.; Ou, J.; Zhang, T.; Zhu, H.; Wu, J., Amphiphilic Copolymeric Micelles for Doxorubicin and Curcumin Co-Delivery to Reverse Multidrug Resistance in Breast Cancer. *J. Biomed. Nanotechnol.* **2016,** 12, (5), 973-985.

29. Quan, Z.; Ying, C.; Wang, X. J.; Xu, J. L.; Zhou, Y.; Wang, S.; Seeberger, P. H.; Jian, Y., Targeted Photodynamic Killing of Breast Cancer Cells Employing Heptamannosylated β-Cyclodextrin-Mediated Nanoparticle Formation of an Adamantane-Functionalized BODIPY Photosensitizer. *ACS Appl. Mater. Interfaces* **2016,** 8, (49), 33405-33411.

30. Wang, X.; Zhang, J.; Cheng, R.; Meng, F.; Deng, C.; Zhong, Z., Facile Synthesis of Reductively Degradable Biopolymers Using Cystamine Diisocyanate as a Coupling Agent. *Biomacromolecules* **2016,** 17, (3), 882.

31. Zhu, C.; Zheng, M.; Meng, F.; Mickler, F. M.; Ruthardt, N.; Zhu, X.; Zhong, Z., Reversibly shielded DNA polyplexes based on bioreducible PDMAEMA-SS-PEG-SS-PDMAEMA triblock copolymers mediate markedly enhanced nonviral gene transfection. *Biomacromolecules* **2012,** 13, (3), 769.

32. Ji, Q.; Qiu, L., Mechanism study of PEGylated polyester and β-cyclodextrin integrated micelles on drug resistance reversal in MRP1-overexpressed HL60/ADR cells. *Colloids Surf., B* **2016,** 144, 203-213.

33. Badwaik, V. D.; Aicart, E.; Mondjinou, Y. A.; Johnson, M. A.; Bowman, V. D.; Thompson, D. H., Structure-property relationship for in vitro siRNA delivery performance of cationic 2-hydroxypropyl-β-cyclodextrin: PEG-PPG-PEG polyrotaxane vectors. *Biomaterials* **2016,** 84, 86.

34. CG, B.; Ellis, L. M., Drug development: Raise standards for preclinical cancer research. *Nature* **2012,** 483, (7391), 531-533.

35. Wu, Y.-L.; Yin, H.; Zhao, F.; Li, J., Multifunctional Hybrid Nanocarriers Consisting of Supramolecular Polymers and Quantum Dots for Simultaneous Dual Therapeutics Delivery and Cellular Imaging. *Adv. Healthcare Mater.* **2013,** 2, (2), 297–301.

36. Swiech, O.; Mieczkowska, A.; Chmurski, K.; Bilewicz, R., Intermolecular Interactions between Doxorubicin and β-Cyclodextrin 4-Methoxyphenol Conjugates. *J. Phys. Chem. B* **2012,** 116, (6), 1765-1771.

37. Shi, Q.; Zhang, L.; Liu, M.; Zhang, X.; Zhang, X.; Xu, X.; Chen, S.; Li, X.; Zhang, J., Reversion of multidrug resistance by a pH-responsive cyclodextrin-derived nanomedicine in drug resistant cancer cells. *Biomaterials* **2015,** 67, 169.

38. Yunomae, K.; Arima, H.; Hirayama, F.; Uekama, K., Involvement of cholesterol in the inhibitory effect of dimethyl-β-cyclodextrin on P-glycoprotein and MRP2 function in Caco-2 cells. *FEBS Lett.* **2003,** 536, (1-3), 225-231.

39. Feng, S.; Hu, Y.; Peng, S.; Han, S.; Tao, H.; Zhang, Q.; Xu, X.; Zhang, J.; Hu, H., Nanoparticles responsive to the inflammatory microenvironment for targeted treatment of arterial restenosis. *Biomaterials* **2016,** 105, 167-184.

40. Liu, J.; Zhong, L.; Zhang, J.; Luo, T.; Zhou, J.; Zhao, X.; Cai, K., Hollow mesoporous silica nanoparticles facilitated drug delivery via cascade pH stimuli in tumor microenvironment for tumor therapy. *Biomaterials* **2016,** 83, 51.

41. Xia, S.; Wen, Y.; Zhu, J. L.; Feng, Z.; Zhang, Z.; Li, J., Thermoresponsive Delivery of Paclitaxel by β-Cyclodextrin-based Poly(N-isopropylacrylamide) Star Polymer via Inclusion Complexation. *Biomacromolecules* **2016,** 17, (12), 3957.

42. Hou, L.; Ma, K.; An, Z.; Wu, P., Exploring the Volume Phase Transition Behavior of POEGA- and PNIPAM-Based Core–Shell Nanogels from Infrared-Spectral Insights. *Macromolecules* **2014,** 47, (3), 1144-1154.

43. Wu, Y.; Liu, X.; Yu, W.; Guo, Z.; Feng, Y., Synthesis and Aggregation Behaviors of Well-Defined Thermoresponsive Pentablock Terpolymers With Tunable LCST. *Macromol. Chem. Phys.* **2012,** 213, (14), 1489–1498.

44. Brockman, K. S.; Lai, B. F. L.; Kizhakkedathu, J. N.; Santerre, J. P., Hemocompatibility of Degrading Polymeric Biomaterials: Degradable Polar Hydrophobic Ionic Polyurethane versus Poly(lactic-co-glycolic) Acid. *Biomacromolecules* **2017,** 18, (8), 2296-2305.

45. Fan, X.; Wang, X.; Cao, M.; Wang, C.; Hu, Z.; Wu, Y.-L.; Li, Z.; Loh, X. J., "Y"-Shape Armed Amphiphilic Star-like Copolymer: Design, Synthesis and Dual-Responsive Unimolecular Micelle Formation for Controlled Drug Delivery. *Polym. Chem.* **2017,** 8, 5611-5620.

46. Fan, X.; Cao, M.; Zhang, X.; Li, Z., Synthesis of star-like hybrid POSS-(PDMAEMA-b-PDLA)8 copolymer and its stereocomplex properties with PLLA. *Mater. Sci. Eng. C* **2017,** 76, 211-216.

47. Li, Z.; Yin, H.; Zhang, Z.; Liu, K. L.; Li, J., Supramolecular Anchoring of DNA Polyplexes in Cyclodextrin-Based Polypseudorotaxane Hydrogels for Sustained Gene Delivery. *Biomacromolecules* **2012,** 13, (10), 3162-3172.

48. Li, Z.; Li, J., Control of Hyperbranched Structure of Polycaprolactone/Poly(ethylene glycol) Polyurethane Block Copolymers by Glycerol and Their Hydrogels for Potential Cell Delivery. *J. Phys. Chem. B* **2013,** 117, (47), 14763-14774.

49. Fan, X.; Wang, Z.; Yuan, D.; Sun, Y.; Li, Z.; He, C., Novel linear-dendritic-like amphiphilic copolymers: synthesis and self-assembly characteristics. *Polym. Chem.* **2014,** 5, (13), 4069-4075.

50. Li, Z.; Zhang, Z.; Liu, K. L.; Ni, X.; Li, J., Biodegradable Hyperbranched Amphiphilic Polyurethane Multiblock Copolymers Consisting of Poly(propylene glycol), Poly(ethylene glycol), and Polycaprolactone as in Situ Thermogels. *Biomacromolecules* **2012,** 13, (12), 3977-3989.

51. Li, Z.; Tan, B. H.; Jin, G.; Li, K.; He, C., Design of polyhedral oligomeric silsesquioxane (POSS) based thermo-responsive amphiphilic hybrid copolymers for thermally denatured protein protection applications. *Polym. Chem.* **2014,** 5, (23), 6740-6753.

52. Alomar, A.; Abdou, S.; De, R. L.; Marsura, A.; Finance, C., Complexation study and anticellular activity enhancement by doxorubicin-cyclodextrin complexes on a multidrug-resistant adenocarcinoma cell line. *Bioorg. Med. Chem. Lett.* **1999,** 9, (8), 1115-1120.

53. Xiang, Y.; Oo, N. N. L.; Lee, J. P.; Li, Z.; Loh, X. J., Recent development of synthetic nonviral systems for sustained gene delivery. *Drug Discovery Today* **2017,** 22, 1318-1335.

54. Yang, D. P.; Oo, M.; Deen, G. R.; Li, Z.; Loh, X. J., Nano-Star-Shaped Polymers for Drug Delivery Applications. *Macromol. Rapid Commun.* **2017**, 1700410.

55. Li, Z.; Tan, B. H.; Lin, T.; He, C., Recent Advances in Stereocomplexation of Enantiomeric PLA-Based Copolymers and Applications. *Prog. Polym. Sci.* **2016,** 62, 22-72.

56. Hwang, J. Y.; Li, Z.; Loh, X. J., Small molecule therapeutic-loaded Liposomes as therapeutic carriers: From development to clinical applications. *RSC Adv.* **2016,** 6, 70592-70615.

57. Li, Z.; Ye, E.; David; Lakshminarayanan, R.; Loh, X. J., Recent Advances of Using Hybrid Nanocarriers in Remotely Controlled Therapeutic Delivery. *Small* **2016,** 35, 4782-4806.

58. Li, Z., How can we fine-tune nanoparticles to improve drug delivery? *Ther. Delivery* **2017,** 8, (8), 597-600.

59. Li, Z.; Loh, X. J., Recent advances of using polyhydroxyalkanoate-based nanovehicles as therapeutic delivery carriers. *Wiley Interdiscip. Rev.: Nanomed. Nanobiotechnol.* **2016,** 9, e1429.

60. Karaduman, D.; Eren, B.; Keles, O. N., The protective effect of beta-1,3-D-glucan on taxol-induced hepatotoxicity: a histopathological and stereological study. *Drug Chem. Toxicol.* **2010,** 33, (1), 8-16.

61. Krol, T., Activity of lysosomal system in mouse liver after taxol administration. *Gen. Pharmacol.* **1998,** 30, (2), 239-243.

62. Guchelaar, H. J.; ten Napel, C. H.; de Vries, E. G.; Mulder, N. H., Clinical, toxicological and pharmaceutical aspects of the antineoplastic drug taxol: a review. *Clin. Oncol.* **1994,** 6, (1), 40-48.

63. Rowinsky, E. K.; Gilbert, M. R.; McGuire, W. P.; Noe, D. A.; Grochow, L. B.; Forastiere, A. A.; Ettinger, D. S.; Lubejko, B. G.; Clark, B.; Sartorius, S. E.; et al., Sequences of taxol and cisplatin: a phase I and pharmacologic study. *J. Clin. Oncol.* **1991,** 9, (9), 1692-1703.

64. Weiss, R. B.; Donehower, R. C.; Wiernik, P. H.; Ohnuma, T.; Gralla, R. J.; Trump, D. L.; Baker, J. R., Jr.; Van Echo, D. A.; Von Hoff, D. D.; Leyland-Jones, B., Hypersensitivity reactions from taxol. *J. Clin. Oncol.* **1990,** 8, (7), 1263-1268.

65. Kingston, D. G.; Snyder, J. P., The quest for a simple bioactive analog of paclitaxel as a potential anticancer agent. *Acc. Chem. Res.* **2014,** 47, (8), 2682-2691.

66. Luong, D.; Sau, S.; Kesharwani, P.; Iyer, A. K., Polyvalent Folate-Dendrimer-Coated Iron Oxide Theranostic Nanoparticles for Simultaneous Magnetic Resonance Imaging and Precise Cancer Cell Targeting. *Biomacromolecules* **2017,** 18, (4), 1197-1209.

Table of Contents Graphic (TOC)